DOI: 10.48011/sbse.v1i1.2212

A Performance Analysis of Transmission Line Differential Protection

Igor F. Prado [*] **Rodrigo P. Medeiros** [**] **Flávio B. Costa** [***] **Kleber M. Silva**[****]

[*] *Department of Exact and Technological Sciences, State University of Santa Cruz, BA, Brazil (e-mail: ifprado@uesc.br).*
[**] *Multidisciplinary Center of Caraúbas, Federal Rural University of the Semi-Arid, RN, Brazil (e-mail: rodrigo.prado@ufersa.edu.br)*
[***] *School of Science and Tecnology, Federal University of Rio Grande do Norte, RN, Brazil (e-mail:flaviocosta@ect.ufrn.br)*
[****] *University of Brasília, DF, Brazil (e-mail: klebermelo@unb.br)*

Abstract: This work accomplishes a comparative analysis between two methodologies of transmission line protections available in commercial relays: percentage and alpha-plane differential protections. In order to verify the operation limits of these protections, several internal and external faults were simulated considering variations of the electrical parameters of fault types, system loading, fault impedance and CT saturation on transmission lines. The fault detection time is strongly influenced by the fault impedance variation, the greater the fault resistance, the longer the time for its detection. Comparing the overall performance of the protections, the alpha plane method showed more accurate and faster responses, since the sequence units are not influenced by the fault impedance.

Keywords: Transmission Line Protection, Percentage Differential Protection, Alpha-Plane Differential Protection.

1. INTRODUCTION

An electric power system is characterized by three major subsystems: generation, transmission and distribution. Transmission lines are important components of the power system since they connect the generation system to the distribution system.

According to brazilian National Electric System Operator (2019), 70% of power system faults occurs on transmission lines due to their length, which makes them more susceptible to weather conditions and vandalism. Therefore, the protection of transmission lines is of utmost importance, since it prevents the spread of the fault to the electrical system by isolating the smallest region with the shortest possible time, as well as reduces equipment damage and ensures system stability, taking into account the fault currents can be several times greater than the steady-state currents and may cause thermal and electrical damage to the equipment. In this way, a fast and reliable transmission line protection operation is required in order to prevent the emergence of faults, which would yield economic losses and major power delivery outages. (Paithankar and Bhide, 2011)

The differential protection is an unitary protection, i.e., it protects the whole line, but it does not protect adjacent equipment. This protection presents several advantages over the distance protection, such as better performance in transmission lines with series compensation and no dependence of the voltage measurement in most applications (Roberts et al., 2001). However, this technique demands a more complex communication system, which increases the implementation costs. (Ziegler, 2012)

With the advent of new digital signal processing techniques and robust communication systems, the differential protection has become a promising alternative for the transmission line protection. Among the differential protection schemes applied in transmission lines, the most traditional is the percentage differential, based on the implementation of electromagnetic relays (Kasztenny et al., 2014). However, the alpha-plane differential protection, which takes into account the ratio between the current phasors that enter and leave a transmission line by using a complex plane, has been commercially applied in the last years (SEL, 2011). This technique was designed to present a more reliable operation when compared to the percentage one, since it provides information about the module and the phase of the local and remote currents.

This paper accomplishes a performance analysis between the transmission line differential protection schemes: percentage and alpha-plane. For this purpose, challenging cases of faults in transmission lines are simulated by varying the type of fault, system loading, fault resistance, and current transformer (CT) saturation. The main objective of this study is to compare the two methods and to verify the behavior in critical situations and operations. The performance of the alpha-plane protection method was slightly higher than the percentage differential protection mainly due to the sequence units.

2. THE TRANSMISSION LINE DIFFERENTIAL PROTECTION PHILOSOPHY

The transmission line differential protection (87L) presents a high degree of selectivity, being capable to ensure the operation in all the extension of the transmission line. The differential protection is based on the comparison of the currents that flow through the terminals of the protected element, providing reliable discrimination between internal and external faults. The protection zone is delimited by the connection of the CTs. During an internal fault condition, for instance, the differential relay sends the trip command for circuit breakers in order to isolate the equipment from the electrical system.

In transmission lines, CTs are usually too far apart. Therefore, a communication system with data synchronization is required to ensure the differential protection operates correctly with the current samples in a same time basis. The synchronization can be performed by means of a communication channel as described in Mills (1991), or by means of the use of external time references, such as the Global Positioning System (GPS) Hall et al. (2003). In this work, phase (87LA, 87LB and 87LC), negative sequence (87LQ) and zero sequence (87LN) units were implemented.

Fig. 1 depicts all the executed steps by the differential protection scheme, per sampling k. From the acquisition of the signal, performed by the CTs, until the tripping command, the following subroutines are executed: the preprocessing step, which consists in performing the digital acquisition of the CT currents using anti-aliasing filters and analog-to-digital converters, as described in Tavares and Silva (2014); the current phasor estimation, used to extract the module and angle of the fundamental component of local and remote currents; and the differential analysis, that implements logics of the percentage- and alpha-plane differential protections.

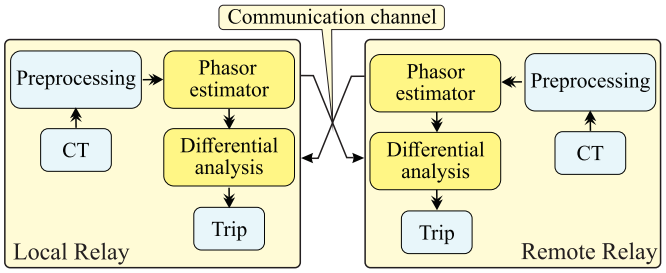

Figure 1. The differential relay block diagram.

2.1 Percentage Differential Protection Algorithm

Fig. 2 depicts the traditional configuration of a percentage differential protection scheme, composed by two CTs, two restriction coils (RC) and one operating coil (OC). Besides the traditional operating coil, the restriction coil has been incorporated into the relay, which has the main function of reinforcing the actuation torque of the relay when an internal fault occurs and weakens it for external faults. (Molas et al., 2012)

According to Fig. 2, CTs have inverted polarities with each other, providing the following analysis based on Kirchhoff current law in the equivalent circuit, in nominal loading or external fault situations, the current phasors ($\hat{I}_L$) and

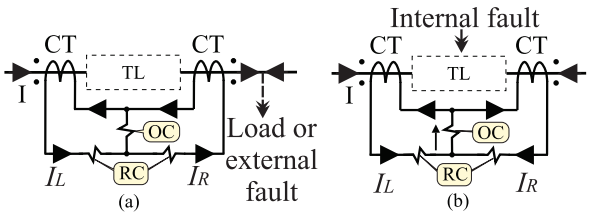

Figure 2. Differential relay: (a) External fault; (b) Internal fault.

($\hat{I}_R$) present the same magnitude and opposite directions, and no current flows in the operating coil, desensitizing the protection (Fig. 2(a)). However, if a fault occurs inside of the protection zone, there is a resulting current flux in the operative coil, which enables the protection operation. The operation and restriction currents (I_{op} and I_{res}) are given by Ziegler (2012):

$$I_{op} = |\hat{I}_L + \hat{I}_R|, \tag{1}$$

$$I_{res} = \frac{|\hat{I}_L - \hat{I}_R|}{2}, \tag{2}$$

where $\hat{I}_L$ and $\hat{I}_R$ are the local and remote terminal currents, respectively. The protection operates when:

$$I_{op} > SLP * I_{res} + k_0, \tag{3}$$

where SLP defines the inclination of the differential characteristic curve; k_0 corresponds to a preset threshold (pickup current). In this application, k_0 is computed taking into account the capacitive current, that arises as a spurious differential current.

The differential characteristic curve is obtained from the solution of (3), with the definitions of the operating and restriction zones (Fig. 3).

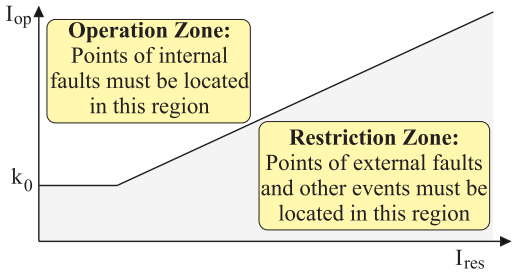

Figure 3. Characteristic curve of the percentage differential protection.Medeiros et al. (2016)

2.2 Alpha-Plane Differential Protection Algorithm

The alpha-plane differential protection is based on the comparison of the ratio between $\hat{I}_L$ and $\hat{I}_R$. Traditionally, the algorithm is defined by a quantity , which is expressed by the ratio between the currents of the local and remote terminals, as follows:

$$\hat{K} = \hat{I}_R / \hat{I}_L. \tag{4}$$

Fig. 4 depicts the alpha-plane differential characteristic, which consists in a circular region centered in the origin

of the complex plane with its respective operation and restriction zones. According to Fig. 4, when the value $\hat{K}$ exceeds the limits of the restriction zone and achieves the operation zone, a internal fault is detected.

Since in external faults or in nominal loading conditions $\hat{I}_L$ is approximately equal to $\hat{I}_R$, but in the opposite direction, as depicted in Fig. 2 (a), the value $\hat{K}$ computed through (4) will be close to the point (-1, 0) in the complex plane, i.e, at the restriction zone (Fig. 4). By the other hand, during an internal fault condition, the real part of $\hat{K}$ becomes positive for internal faults, and negative within circumference $R_2 = 1/R_1$ for outfeed faults (Fig. 4). The region called *"rainbow"* was choosed according to Roberts et al. (2001) and the operation and restriction zones were defined according to Benmouyal and Lee (2004), taking into account the effects of the communication delays, capacitive currents and CT saturation.

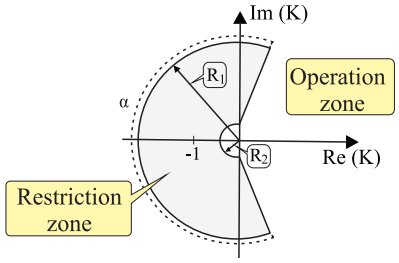

Figure 4. Characteristic curve of the alpha-plane differential protection.

3. METHODOLOGY

The modeling of the 230 kV power system shown in Fig. 5, was performed using the Matlab/Simulink software. The protected transmission line (T12), was represented by distributed parameter model of Bergeron. Coupling capacitor voltage transformers (CCVTs) and current transformers (CTs) were positioned in both line terminals and their models can be seen in IEEE-PSRC (2004). A typical 60 db SNR (Signal-to-Noise-Ratio) was considered at the measured signals to make them more realistic. The system-to-line impedance ratio (SIR) was choosed to be equal to 0.1 at local and remote terminals, and the power system loading angle was equal to -15, which corresponds to a moderate power.

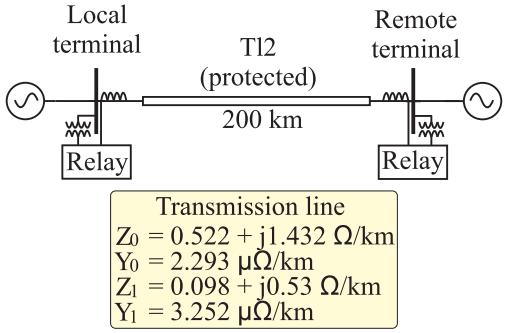

Figure 5. Power system model.

The currents were sampled with a sampling rate of 15.36 kHz, and filtered through a second-order Butterworth anti-aliasing low-pass filter, with cutoff frequency of 960 Hz. After the analog filtering, the signals were subsampled to a sampling rate of 960 Hz, value commonly used in commercial relays which corresponds to 16 samples per cycle of 60 Hz, and then the phasors were estimated by means of the one-cycle Fourier algorithm.

The effect of the communication channel was considered taking into account a delay in the samples sent from each terminal in accordance with the communication protocol described in Hou and Dolezilek (2010). The times considered to represent the message processing in the communication device and the transmission of the signal through the optical fiber in a length of 200 km (length of the line) were 3 ms and 2 ms, respectively, in accordance with Costa et al. (2017). Therefore, the total communication delay was 5 ms.

Tables 1 and 2 describes the databases with the fault parameters that were varied to performance assessment of the differential protections, considering the presence and absence of CT saturation. All simulated cases were obtained by changing only one parameter at time, while the others were maintained in their default values, namely: fault inception angle of $\theta_f = 0°$, fault resistance of $r_f = 0$ Ω, and fault location at $d_f = 100$ km.

Therefore, the total number of internal fault cases is 1008, considering the combination of 4 types of fault, 101 fault resistance values, 25 loading angles, and 2 saturation conditions. The total cases of external faults is 176, considering 4 types of faults, 11 fault resistance values, 2 application sites and 2 saturation conditions.

Table 1. Configuration for internal faults

Simulation variables	Values
Fault type	AG, AB, ABG, ABC.
Fault resistance $r_f(\Omega)$	$0 < r_f < 1000$ ($\Delta r_f = 10\Omega$)
System loading $\delta_l(°)$	-120, -110°, ..., 110°, 120°.
Total	1008 scenarios

Table 2. Configuration for external faults

Simulation variables	Values
Fault type	AG, AB, ABG, ABC.
Fault resistance $r_f(\Omega)$	$0 < r_f < 500$ ($\Delta r_f = 50\Omega$)
Fault location d_f	External local and remote terminal
Total	176 scenarios

4. RESULTS

The following results show the behavior of the phase and sequence units for single-phase faults, emphasizing that their behavior can be extended to the analysis of other types of faults.

4.1 External faults

Fig. 6 depicts the trajectory of the operating points of phase and sequence units, in a single line-to-ground external fault in the presence and in the absence of CT saturation.

With respect to the percentage differential protection, the units presented higher sensitivity during CT saturation. According to Figs. 6(a), (c) and (e), the operation points related to the external fault without CT saturation remained at the restriction zone during all the event, whereas

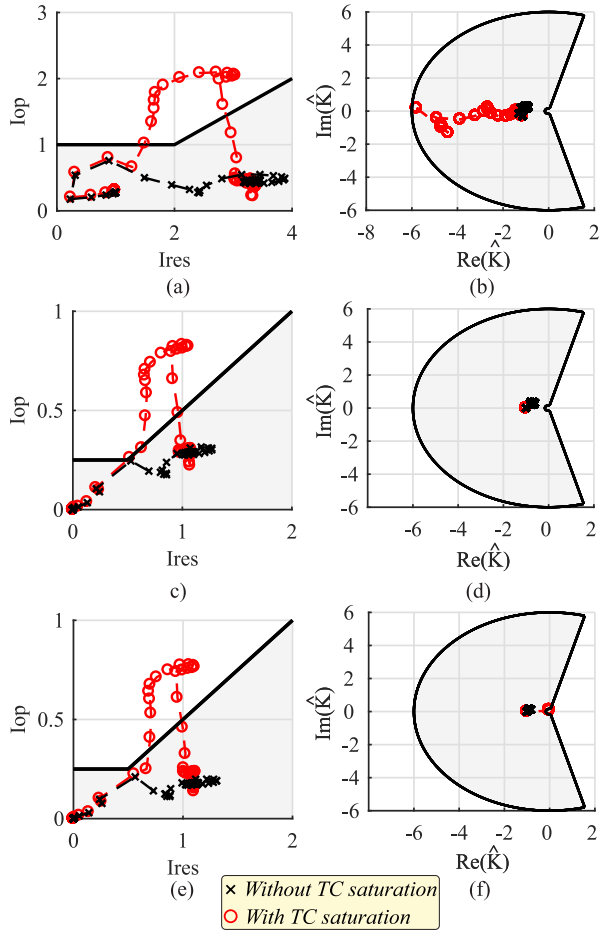

Figure 6. External fauts: (a) Percentage 87LA; (b) Alpha-plane 87LA; (c) Percentage 87LG; (d) Alpha-plane 87LG; (e) Percentage 87LQ; (f) Alpha-plane 87LQ.

the most of the operation points moved to the operation zone during external fault with CT saturation, which could cause relay misoperation. This fact is expected since the CT secondary signals are distorted during CT saturation, causing the measurements at the line terminals very different from each other and allowing the differential protection to act improperly.

Regarding the alpha-plane method, the 87LG and 87LQ units did not show significant variation during CT saturation, and the 87LA was more affected. However, all operating points of the 87LA unit remained in the restriction zone and no trip was provided. During external faults, even under saturation condition, the ratio K moves in the negative direction within the restriction zone.

4.2 Internal single-phase-to-ground fault with CT saturation

Fig. 7 depicts the trajectory of the operating points of phase and sequence units, in a single line-to-ground internal fault in the presence and in the absence of CT saturation. The fault was simulated with $d_f = 100$ km, $r_f = 0\ \Omega$, and $\theta = 0^o$. After CT saturation initiation, the trajectory performed by the operating points in the operation and restriction zones of both percentage differential and alpha-plane protection methods is affected. Regarding the percentage differential method, the saturation of the CT altered the trajectory in order to increase the restriction current, due to the restriction coils, however there was no reduction in the operating current, therefore the entire trajectory remained in the restriction zone. With respect to the alpha-plane method and unlike the percentage differential method, CT saturation caused a change in the magnitudes of the currents such that the operation points moved to the restriction region [Figs. 7(b), (d), and (f)] in all units. At the end of the CT saturation period, the points returned to the operation region. Therefore, relay tripping was delayed due to the CT saturation.

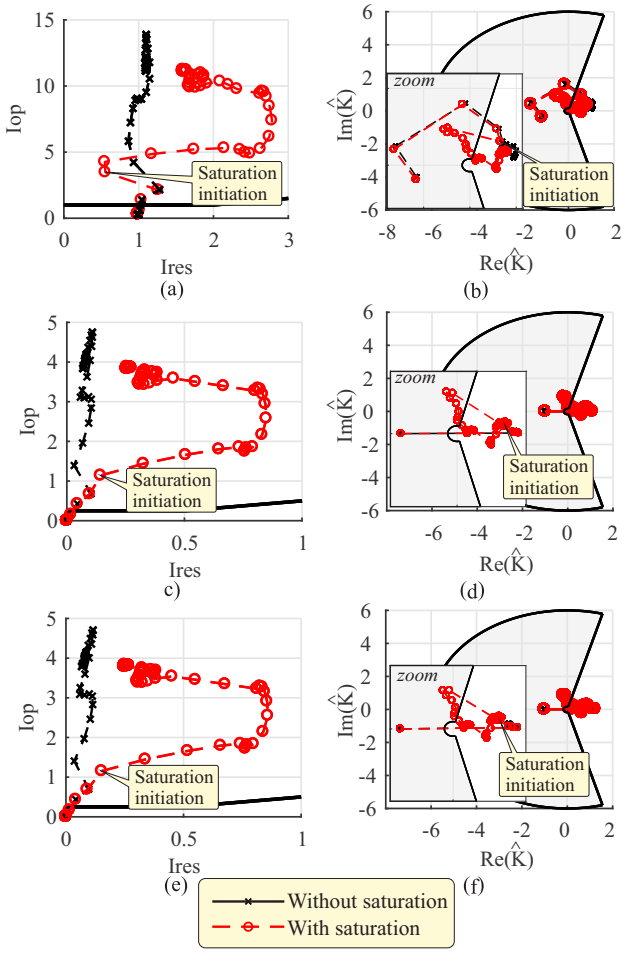

Figure 7. Internal single-phase-to-ground fault: (a) Percentage - 87LA unit; (b) Alpha-plane - 87LA unit; (c) Percentage - 87LG unit; (d) Alpha-plane - 87LG unit; (e) Percentage - 87LQ unit; (f) Alpha-plane - 87LQ unit.

4.3 System load analysis

This section assess the impact of the system loading variation on the performance of the two protection methods. For this analyze, it was assumed the remote and local bars had voltages equal to $1\angle 40^o$ p.u. and local bar with $1\angle \delta_L{}^o$ p.u. The phase of the voltage of the local bar was varied between -120^o and 120^o in order to verify the effects of the load system variation. The power flow moves from bars with larger angles to bars with smaller angles and it is proportional to the angular opening between them.

An idea about the performances of the percentage- and alpha-plane differential protection methods regarding the

system load variation is depicted in Fig. 8. For sake of illustration, the most representative point of operation in the post-fault regime was represented for each analyzed case.

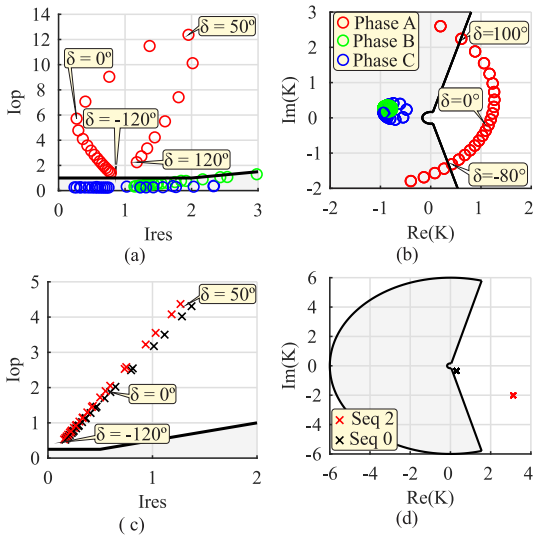

Figure 8. System loading - Internal AG fault: (a) Percentage - Phase units; (b) Alpha-plane - Phase units; (c) Percentage - Sequence units; (d) Alpha-plane - Sequence units.

According to Figs. 8(a) and (b), for $\delta_L > 40$, the power flow direction is from local terminal to remote terminal and the operating current increases. Otherwise, if $\delta_L < 40$, the power flow is in the opposite direction, causing a reduction of the operating current and in the ratio $\hat{K}$, according to (4). The success rates for the phase units of the percentage- and alpha plane methods were 100% and 75%, respectively. Regarding the sequence units, both methods were not affected by the system loading variation, ensuring success rate of 100% [Figs. 8(c) and (d)].

4.4 Detection time analysis

The fast action of protection is desirable in an electrical power system as it prevents and reduces damage to equipment and ensures the stability of the system.

Fig. 9 depicts the most representative post-fault points for single-phase-to-ground faults simulated with variation of the fault resistance parameter, for the phase and sequence units of the percentage differential protection method. In a general way, the sensibility of the units decreased with the increase of the fault resistance. However, the sequence units were less affected than the phase unit. The effect of delay in relay operation for these faults is depicted in Fig. 10. According to Fig. 10, the greater the fault resistance, the longer the detection time and the delay in operation. It is noteworthy that the percentage differential protection has not been able to identify faults with resistances greater than 885 Ω.

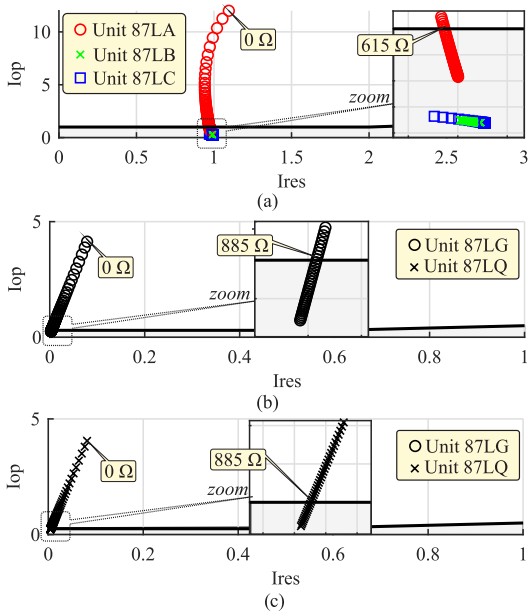

Figure 9. Percentage differential - Parametric trajectory for single-phase faults: (a) Phase units; (b) Zero sequence unit; (c) Negative sequence unit.

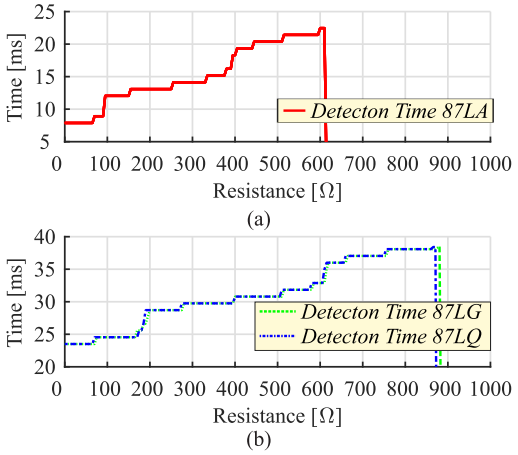

Figure 10. Fault detection time for fault impedance variation: (a) 87LA unit; (b) 87LG and 87LQ units.

Fig. 11 shows the parametric analysis of the same cases considering the alpha-plane differential protection scheme. The 87LA unit has a lower sensitivity when compared to the percent differential protection phase unit, since the fault detection limit is 550 Ω. However, the sequence units do not lose sensitivity, ensuring 100% of the detection cases simulated. Fig. 12 depicts the relationship between the fault impedance and the detection time. The detection time increases with the increase of the fault impedance for all units.

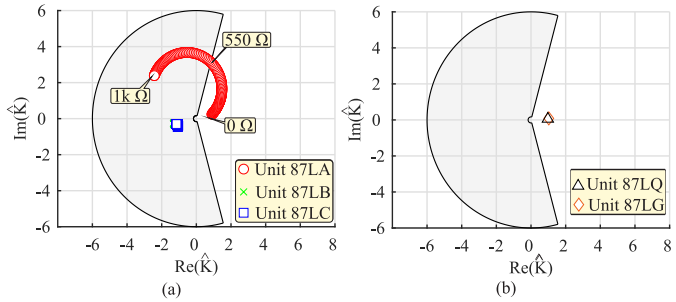

Figure 11. Alpha-plane - Parametric trajectory for single-phase faults. (a) Phase units; (b) Zero and negative sequence units.

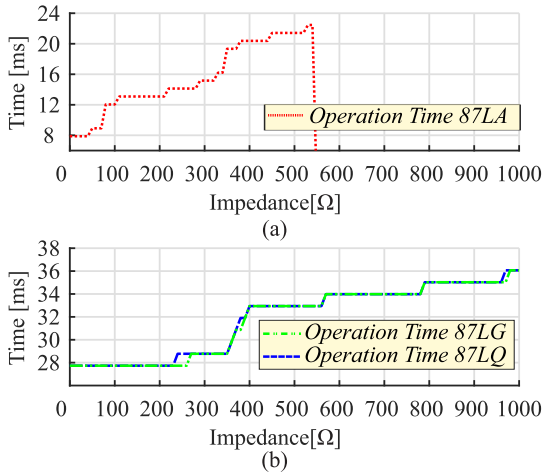

Figure 12. Fault detection time for fault impedance variation: (a) 87LA unit; (b) 87LG and 87LQ units.

5. CONCLUSION

This paper presented a comparison study between the performances of two transmission line differential protection algorithms: the percentage and alpha-plane methods. Several simulated internal and external faults, with variations of the fault type, fault resistance, and system loading, in the presence and in the absence of CT saturation, was considered. In a general way, both strategies presented a fast fault detection. However, the fault resistance variation greatly affects the permanent regime point of the phase units of both methods and of the sequence units of the percentage method, a fact not observed in the alpha plane sequence units, therefore according to this feature, the alpha-plane method reached a 100% fault detection rate, while the percentage method reached 95.3%. It is noteworthy that the greater the fault resistance, the greater the time spent for its identification.

The studies of saturation and loading of the system point out the need for extra routines that could assist in increasing safety in order to identify the saturation of CTs during external faults mainly in the percentage method most affected by this aspect. For the case of the variation of the loading of the system, it is possible to rotate the restriction and operation zones for the alpha plane method, that was affected by this aspect.

The study performed in this work is important for the understanding of methodologies and aspects that affect the safety and reliability of a differential protection system for transmission lines, where the percentage differential protection presented limitations mainly in the identification of high impedance faults, whereas the alpha-plane method was the most robust and presented the fastest response.

ACKNOWLEDGMENT

This work was supported by the National Council for Scientific and Technological (CNPq) and by the Coordination for the Improvement of Higher Education Personnel (CAPES), Brazil.

REFERENCES

Benmouyal, G. and Lee, T. (2004). Sequence-current differential elements. *SEL Journal of Reliable Power*.

Costa, F.B., Monti, A., Lopes, F.V., Silva, K.M., Jamborsalamati, P., and Sadu, A. (2017). Two-terminal traveling-wave-based transmission-line protection. *IEEE Transactions on Power Delivery*, 32(3), 1382–1393. doi:10.1109/TPWRD.2016.2574900.

Hall, I., Beaumont, P.G., Baber, G.P., Shuto, I., Saga, M., Okuno, K., and Uo, H. (2003). New line current differential relay using gps synchronization. In *2003 IEEE Bologna Power Tech Conference Proceedings,*, volume 3, 8pp. doi:10.1109/PTC.2003.1304464.

Hou, D. and Dolezilek, D. (2010). Iec 61850 – what it can and cannot offer to traditional protection schemes. *SEL Journal of Reliable Power*, 1(2), 1–11.

IEEE-PSRC (2004). Emtp reference models for transmission line relay testing.

Kasztenny, B., Benmouyal, G., Altuve, H., and Fischer, N. (2014). Tutorial on operating characteristics of microprocessor-based multiterminal line current differential relays. *Line Current Differential Protection: A Collection of Technical Papers Representing Modern Solutions*.

Medeiros, R.P., Costa, F.B., , and Almeida, M.A.D. (2016). Assessment of the main phasor-based power transformer differential protection elements. *SBSE - VI Simpósio Brasileiro de Sistemas Elétricos*.

Mills, D.L. (1991). Internet time synchronization: the network time protocol. *IEEE Transactions on Communications*, 39, 1482–1493.

Molas, E.C., Silva, K.M., and Kusel, B.F. (2012). Teoria de comparadores aplicada na avaliação da atuação da proteção diferencial de linhas de transmissões no plano alfa. *XIX CBA Congresso Brasileiro de Automática*.

Paithankar, Y.G. and Bhide, S. (2011). *Fundamentals of power system protection*. PHI Learning Pvt. Ltd.

Roberts, J., Tziouvaras, D., Benmouyal, G., and Altuve, H. (2001). The effect of multiprinciple line protection on dependability and security. In *proceedings of the 55th Annual Georgia Tech Protective Relaying Conference, Atlanta, GA*.

SEL, S.E.L. (2011). Sel-411l: Advanced line differential protection, automation, and control system. URL `https://selinc.com/products/411L/`.

Tavares, K.A. and Silva, K.M. (2014). Evaluation of power transformer differential protection using the atp software. *IEEE Latin America Trans.*, 12(2), 161–168. doi:10.1109/TLA.2014.6749533.

Ziegler, G. (2012). *Numerical Differential Protection: Principles and Applications*. John Wiley & Sons.